Catalysis Today 147S (2009) S24–S29

Contents lists available at ScienceDirect

Catalysis Today

journal homepage: www.elsevier.com/locate/cattod

# Towards the rationalization of the washcoating process conditions

Cinzia Cristiani [a,*], Carlo Giorgio Visconti [b], Elisabetta Finocchio [c], Paola Gallo Stampino [a], Pio Forzatti [b]

[a] *Politecnico di Milano, Dipartimento di Chimica, Materiali e Ingegneria Chimica "Giulio Natta", Piazza Leonardo da Vinci 32, 20133 Milano, Italy*
[b] *Politecnico di Milano, Dipartimento di Energia, Piazza Leonardo da Vinci 32, 20133 Milano, Italy*
[c] *Università degli Studi di Genova, Dipartimento di Ingegneria Chimica e di Processo, Piazzale J.F. Kennedy 1, 16129 Genova, Italy*

ARTICLE INFO

*Article history:*
Available online 3 August 2009

*Keywords:*
Washcoating
Catalysts preparation
Alumina
Structured catalysts

ABSTRACT

The effects on the slurry rheology of the chemical composition of suspensions representative of those typically adopted for the washcoating of structured supports have been studied in this work, with the purpose of rationalizing the process conditions used in the preparation of structured catalysts. It has been found that the viscosity of the suspensions can be easily predicted and controlled by knowing the pore volume and the nature of the surface of the dispersed powders. In order to prepare suspensions, containing different powders, with the same rheology, water content has to be modulated considering the pore volume, while the dispersant (nitric acid) amount has to be proportional to the quantity required by the complete charging of the surface of the dispersed powders. Obtained results clarify some fundamentals of the washcoating processes and allow a dramatic reduction of the number of experimental tests typically performed to washcoat a structured support starting from a new catalytic material.

## 1. Introduction

Washcoated structured catalysts consist in metallic or ceramic structures in the form of honeycomb monoliths, plates or foams, coated with layers of catalytically active materials (washcoat).

Due to their unique properties, washcoated honeycomb monoliths have become since many years the standard catalyst shape in most applications of environmental catalysis [1–3]. In fact, the possibility to dramatically reduce the pressure drops compared to traditional packed bed reactors, while keeping the surface area very high, makes them optimal for the application where the reactants are highly diluted and the energy efficiency can be determinant.

More recently, in addition, the application of monolithic catalysts has been proposed as a way for the intensification of some classical processes of the industrial chemistry, like the gas/solid endo-exothermal reactions [4–6]. In these situations, in fact, the adoption of structured catalysts with highly conductive supports permits to remove (in the case of exothermic processes) or supply (in the case of endothermic processes) easily the heat of reaction, allowing to run these processes on the industrial scale with small temperature gradients both in the axial and in the radial directions, with specific productivities similar or higher with respect to conventional reactors.

Different techniques are used to deposit the washcoat layers onto structured supports; among them, dip-coating [7] and dip-blowing [8] are the methods most widely proposed at the lab-scale since they are relatively simple and allow to obtain uniform coatings. Anyway, all the washcoating techniques require the use of stable dispersions with appropriate rheological properties [7–9]: this result can be obtained using colloidal dispersions or colloid-containing suspensions. The presence of a certain amount of colloid, in fact, guarantees the stability of the suspensions and governs the rheological behaviour [9,10]. For instance, in the case of alumina powders, one of the most studied materials, stable suspensions can be easily obtained using a monoprotic acid as dispersant and a ball-milling process for the reduction of the particles size [9].

Although a lot of papers have been published about the washcoating procedure of structured supports, available data mainly refer to the preparation of specific materials or are related to particular applications.

With the aim of rationalizing the choice of the process conditions adopted in the washcoating of structured supports, an investigation has been undertaken in our labs analysing the correlation existing between the morphology and the nature of the surface of the suspended materials and the rheological properties of the obtained slurries. It is well known, in fact, that the final properties of the washcoated layer are strongly related to the rheological properties of the suspension [7].

Specifically, data on some alumina and alumina-based materials are reported and discussed in this paper. Obtained results are

---

[*] Corresponding author. Tel.: +39 02 23993248; fax: +39 02 70638173.
*E-mail address:* cinzia.cristiani@polimi.it (C. Cristiani).

0920-5861/$ – see front matter © 2009 Elsevier B.V. All rights reserved.
doi:10.1016/j.cattod.2009.07.031

considered as fundamentals for the study of more complex materials such as metal-supported catalysts. The final goal is to find simple rules to determine *a priori* the slurry composition required to reach the desired rheological behaviour.

## 2. Experimental

### 2.1. Characterization of the materials

Five alumina samples (Puralox, PuraloxL3, Siralox, Pural KRI and Pural KRII supplied by Sasol Chemie) were investigated (Table 1). Puralox, PuraloxL3, Siralox were used as received, while Pural KRI and KRII were calcined at 800 °C in flowing air for 10 h (heating and cooling rates 2 °C/min).

Surface area and pore volume were determined by nitrogen adsorption–desorption at 77 K (Micromeritics Tristar 3000 instrument). Pore volume was also determined by water adsorption after drying the powders overnight at 110 °C in recirculating air.

X-ray diffraction analyses were carried out on a Philips instrument with vertical goniometer PW 1050/70 (Ni-filtered Cu K$\alpha$, $2\theta$ range = 20–70°, step scan 0.05°, time step = 12 s).

Powder surface characterization was performed both by a titration method and FT-IR spectroscopy of adsorbed probe molecules.

Maximum surface charging of the adopted materials was determined according to the titration methodology reported in [11]. In a typical experiment, 8 g of powder are inserted in a closed reactor pre-loaded with 200 $cm^3$ (V) of an aqueous solution at given pH ($pH^{start}$); the powder is kept under stirring at a constant temperature and the pH value is recorded as a function of time, until pH reaches an asymptotic value ($pH^{end}$). The surface charging ($q$) is determined by means of Eq. (1)

$$q = F * \Delta H^+ * m^{-1} * S_{BET}^{-1} \quad (1)$$

where $F$ the Faraday constant, $m$ the amount of powder (g), $S_{BET}$ the surface area ($m^2/g$) and $\Delta H^+$ the variation of the moles of $H^+$ ions in solution, calculated according to Eq. (2):

$$\Delta H^+ = (10^{-pH^{start}} - 10^{-pH^{end}})V \quad (2)$$

The maximum surface charging corresponds to the asymptotic value of the $H^+$ adsorbed by the material upon decreasing the value of $pH^{start}$.

The pH measurements were performed with a pH-meter (Metrohm Titrino 719S) equipped with a combined sensitive glass electrode.

The presence of dissolution phenomena, due to the presence of the solid in contact with a strong acid medium, was checked by analysing the filtered solution collected after the reaction. Only negligible amounts of ions (0.5%, w/w, of the total) were found.

Surface nature of the adopted materials was characterized by FT-IR spectroscopy with probe molecules. FT-IR spectra have been recorded by Nicolet 380 FT instrument, using a conventional IR cell connected to a gas manipulation apparatus. The sample powders were pressed into self-supporting disks of around 30 mg and activated in vacuum at 500 °C prior to each adsorption experiment. Pivalonitrile (PN) adsorption allowed the evaluation of the surface acid sites, while $CO_2$ adsorption was used to test the presence and the nature of nucleophilic centres (i.e. incompletely coordinated hydroxy groups and oxide anions), analyzing the formation of a mixture of hydrogen carbonate and carbonate surface species. PN was supplied by Aldrich, $CO_2$ was supplied by SIAD.

**Table 1**
Adopted materials.

| Commercial name | Acronym | Composition | SA[a] ($m^2/g$) | PV[b] ($cm^3/g$) | PS[c] ($\mu m$) |
|---|---|---|---|---|---|
| Pural KRI | PALI | $\gamma$-$Al_2O_3$ | 153 | 1.21 | 18 |
| Pural KRII | PALII | $\gamma$-$Al_2O_3$ | 153 | 1.17 | 18 |
| Puralox SCFa 140 | POX | $\gamma$-$Al_2O_3$ | 140 | 0.54 | 18 |
| Puralox SCFa 140 L3 | POXL3 | 3 wt% La/$\gamma$-$Al_2O_3$ | 138 | 0.56 | 18 |
| Siralox | SOX | 5 wt% Si/$\gamma$-$Al_2O_3$ | 147 | 0.81 | 19 |

[a] SA = Surface area.
[b] PV = Pore volume.
[c] PS = Particle size after ball-milling.

### 2.2. Characterization of the slurries

Slurries were prepared according to the ball-milling procedure reported elsewhere [7]. The powders were suspended in deionized water and nitric acid was used as dispersant. Zirconium oxide spheres were used as grinding bodies. The suspensions were ball-milled for 24 h at 50 rpm.

The rheological behaviour of the obtained suspensions was analysed at 20 °C by means of a rotational rheometer (Reologica Instruments Stresstech 500) equipped with a 40 mm flat-plate. Shear rates between 1 and 100 $s^{-1}$ were investigated at constant shear stress.

The granulometry of the original and suspended powders was measured by means of a laser particle size analyser (Cilas 1180).

## 3. Results and discussion

The characteristics of the adopted powders and the corresponding labels are reported in Table 1.

All the samples consist of $\gamma$-$Al_2O_3$ phase with similar surface areas (140–150 $m^2/g$) and pore volumes varying from 0.54 and 1.21 $cm^3/g$. Before the milling, in addition, all the materials are characterized by bimodal distributions with maxima at 50 and 10 $\mu$m. The milling process reduces the average dimension of the particles and, after the milling process, monomodal distributions centred at 18–19 $\mu$m are found for all the samples. Accordingly, in the following, both the phase composition and the particles dimensions will not be further discussed being the same for all the considered samples.

### 3.1. Effect of the pore volume

Supports with similar chemical nature and different pore volume (POX, PALI, PALII) were suspended using the same recipe, i.e. the same water/powder and acid/powder ratios (1.4 g/g and 2.16 mmol/g, respectively), and ball-milled for 24 h.

Obtained slurries were found to have different rheological behaviours: in the case of POX, a stable suspension with a non-Newtonian shear-thinning behaviour and a viscosity of about 0.04 Pa*s (at shear rate 10 $s^{-1}$) was obtained. On the contrary, PALI and PALII formed a fluid with a viscosity too high to be measured.

Slurries with constant acid content and different water/powder ratios were prepared to evaluate how pore volume could affect their rheological behaviour. The total amount of water was modulated so that the "external" water (defined as the total content of water minus the powder pore volume) was the same in all the samples (Table 2).

Rheological behaviours for the samples with the same external water are reported in Fig. 1. Similar viscosity values (Table 2) were obtained for the different samples. In particular the rheological curves of alumina PALI and PALII were found to be almost superimposed and very close to that of POX. The observed differences are consistent with the experimental error in measuring such low viscosities.

Thus, in the case of samples with the same chemical composition and structure, once fixed the dispersant/powder

**Table 2**
Viscosity at shear rate 10 $s^{-1}$ of slurries containing materials with the same chemical nature.

| Powder | $H_2O$/p (g/g) | $H_2O_{external}$/p[a] (g/g) | $HNO_3$/p (mmol/g) | Viscosity (Pa s) |
|---|---|---|---|---|
| PALI | 2.07 | 0.86 | 2.16 | 0.02 |
| PALII | 2.03 | 0.86 | 2.16 | 0.02 |
| POX | 1.40 | 0.86 | 2.16 | 0.04 |

p = Powder.
[a] $H_2O_{external}$/p = $H_2O$/p-PV.

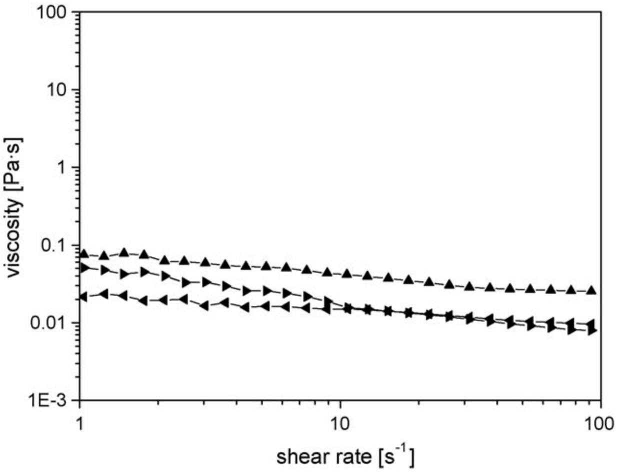

**Fig. 1.** Rheological behaviour of the prepared slurries (recipes reported in Table 2). (▲) POX; (▶) PALI; (◀) PALII.

ratio, the amount of "external water", i.e. water not adsorbed in the particles pores, is the parameter controlling the viscosity.

A similar analysis was performed on samples with the same structure ($\gamma$-$Al_2O_3$), but with different composition, i.e. POX, POXL3 and SOX. POX and POXL3 have similar pore volume, 0.54 and 0.56 $cm^3$/g respectively, while SOX shows a pore volume considerably higher, being equal to 0.81 $cm^3$/g.

In line with the results discussed above, the suspension of SOX was prepared by adding an amount of water corrected to obtain the same "external" water of the POX and POXL3 suspensions, while the $HNO_3$/powder ratio was kept constant at 2.16 mmol/g (Table 3). The corresponding flow curves are reported in Fig. 2. It is evident that despite the same "external" water content in the slurry, the viscosity of silica-doped alumina is still 1–2 orders of magnitude higher than that of undoped and lantana-doped samples.

Thus, in the case of materials with different chemical nature, the pore volume cannot be the only parameter to be considered for the formulation of the recipe of the slurries.

**Table 3**
Slurry recipes and surface charging of the suspended powders.

| Powder | Symbol | $H_2O$/p (g/g) | $H_2O_{external}$/p[a] (g/g) | $HNO_3$/p (mmol/g) | MSC[b] ($C/m^2$) |
|---|---|---|---|---|---|
| POX | ▲ | 1.40 | 0.86 | 2.16 | 1.04 |
| POXL3 | ● | 1.40 | 0.84 | 2.16 | 1.06 |
| SOX | ■ | 1.40 | 0.59 | 2.16 | 0.71 |
| SOX | □ | 1.65 | 0.86 | 2.16 | 0.71 |
| SOX | ◇ | 1.65 | 0.86 | 1.47 | 0.71 |

p = Powder.
[a] $H_2O_{external}$/p = $H_2O$/p-PV.
[b] MSC = Maximum surface charging.

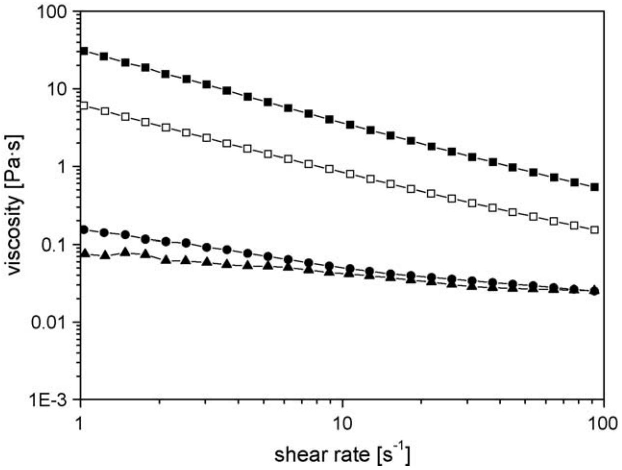

**Fig. 2.** Rheological behaviour of the prepared slurries (recipes and symbols reported in Table 3). Squares = SOX; triangles = POX; circles = POXL3.

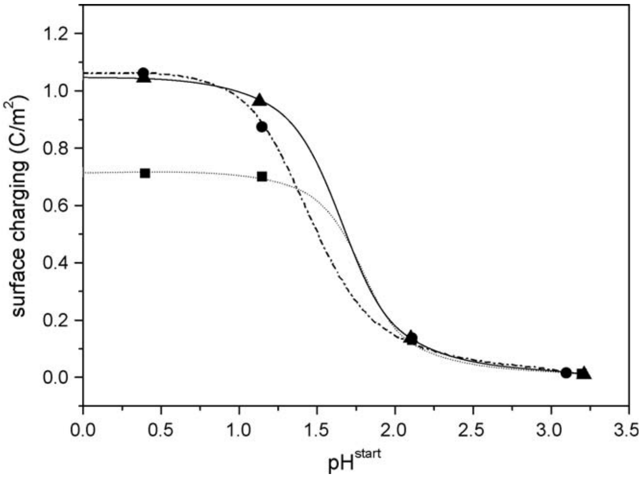

**Fig. 3.** Determination of the maximum surface charging. (▲) POX, (●) POXL3, (■) SOX. Lines are drawn as guide for the eyes.

### 3.2. Effect of the chemical nature

Apart from the water/powder ratio, the other parameter controlling the viscosity of the slurries is the dispersant content, in this case $HNO_3$ [7]. Accordingly, the interactions between the $HNO_3$ and the different alumina, namely POX, POXL3 and SOX, were studied at constant external water content.

The surface charging values at fixed pH were determined according to the titration method described in the experimental section. Results are plotted in Fig. 3, while the maximum surface charging values are reported in Table 3. It is evident that both the undoped (POX) and the La-doped (POXL3) alumina show similar maximum surface charging values, while the Si-doped material (SOX) shows a surface charging significantly lower. This means that the amount of acid required to completely charge the Si-doped alumina is considerably lower than the amounts required to charge POX and POXL3 samples.

It is reported in the literature that free hydrogen ($H^+$) ions could catalyse reactions of colloid reticulation that result in a viscosity increase [12]. This increase is due to the beginning of cross-linking reactions between the particles that progressively induce the formation of a gel, as a consequence of the sol–gel transition. Accordingly, the higher viscosity of SOX sample could be due to the

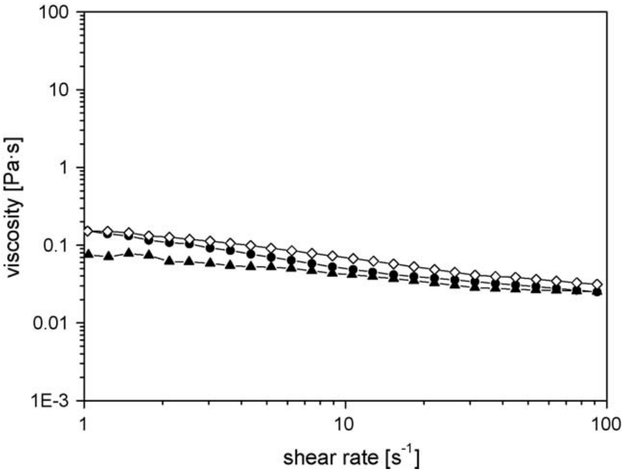

**Fig. 4.** Rheological behaviour of the prepared slurries (recipes and symbols reported in Table 3). Diamonds = SOX; triangles = POX; circles = POXL3.

acid used for the preparation of the slurry, in excess to that required for the total surface charging.

On these bases, slurries of POX, POXL3 and SOX were prepared by calculating the total water content considering the pore volume and the amount of acid considering the surface charging. In particular, an amount of nitric acid proportional to that added in the case of POX (and POXL3) by a factor equal to the ratio between the MSC of POX and MSC of SOX was added. In symbols:

$$\left(\frac{HNO_3}{\text{powder}}\right)_{SOX} = \left(\frac{HNO_3}{\text{powder}}\right)_{SOX}\left(\frac{MSC_{SOX}}{MSC_{POX}}\right) \qquad (3)$$

In Fig. 4 the flow curves of these suspensions are reported. The curves of the 3 different alumina are substantially overlapped. Therefore, in the case of materials with different chemical nature, the acid content must be modulated considering the maximum surface charging of the dispersed powder. More in general, slurries with similar viscosities, containing different materials (with different chemical composition and pore volume), can be obtained by suspending the powders with a fixed amount of "external" water and an amount of acid proportional to the maximum surface charging by a constant factor. This because the relevant parameters controlling the viscosity of the suspensions are the amount of free water, i.e. the water not adsorbed in the pores of the particles, and the charge of each suspended particle. The former parameter (the external water) depends on the total amount of water added to the powders and on their pore volume; the latter (the surface charge) depends on the amount of added acid and on the maximum surface charging of the material.

### 3.3. Nature of the surface

The evaluation of the surface charging via acid titration is a useful methodology to calculate *a priori* the total amount of acid to be used in the formulation of slurries for washcoating processes. However, this method does not provide any explanation concerning the reasons why different materials show different or similar surface charging. In order to comprehend the results collected with the titration method, the nature of the surface of POX, POXL3 and SOX samples was investigated by means of FT-IR analysis.

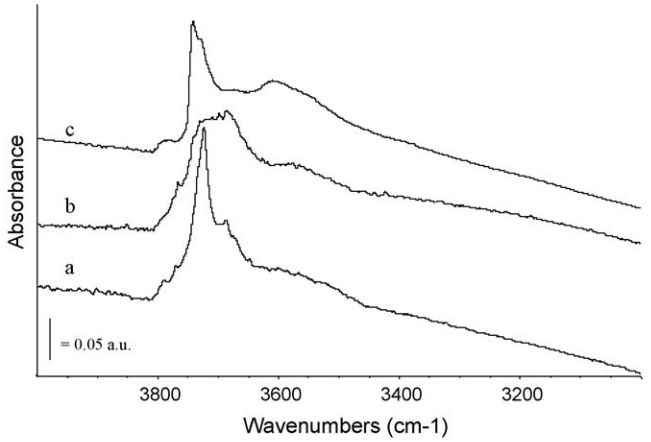

**Fig. 5.** FT-IR spectra of POX (a), POXL3 (b) and SOX (c) samples outgassed at 773 K. OH stretching region.

The infrared spectra of the POX sample in the OH stretching region following outgassing at 500 °C shows typical features due to OH bands of partially dehydroxylated alumina at 3790, 3770, and 3720 cm$^{-1}$, strong (Fig. 5a). These bands are assigned to terminal OHs over two different tetrahedrally coordinated Al ions and over octahedrally coordinated Al ions, respectively. Broad components at 3680 and 3580 cm$^{-1}$ are due to bridging and triple bridging OH groups [13].

Following $La_2O_3$ addition (sample POXL3, Fig. 5b) the OH region spectrum shows one strong and complex band centred at 3720 cm$^{-1}$ and tailing towards lower frequencies, with a weak shoulder at 3770 cm$^{-1}$, due to residual alumina OHs. New components at lower wavenumbers are responsible for the broadening of the main peak in this region. This effect is consistent with data reported by Cui et al. [14] which ascribed the shift of the OH bands in Al–La materials spectra to the formation of new OH species, likely La–OH. On the other side, for such a lower lanthanum content, we cannot detect isolated La–OH species, whose stretching has been reported by several authors in the range 3680–3590 cm$^{-1}$ [15,16].

The SOX sample spectrum (Fig. 5c) shows, in addition, another sharp component at 3740 cm$^{-1}$, characterizing surface silanols groups as expected for silica-containing materials.

The adsorption of $CO_2$, a weakly acidic probe molecule, over the three surfaces leads to the spectra reported in common scale in Fig. 6 (the gas phase $CO_2$ spectrum has been subtracted).

On SOX surface (Fig. 6a) three main broad bands can be detected with maxima at 1645 cm$^{-1}$, tailing towards lower frequencies, 1462 and 1232 cm$^{-1}$, assigned to adsorbed hydrogen carbonated species. Traces of carbonate species could also been detected, characterized by shoulders of the main bands at 1480 and 1600 cm$^{-1}$. Physisorbed (weakly adsorbed) $CO_2$ is also detectable

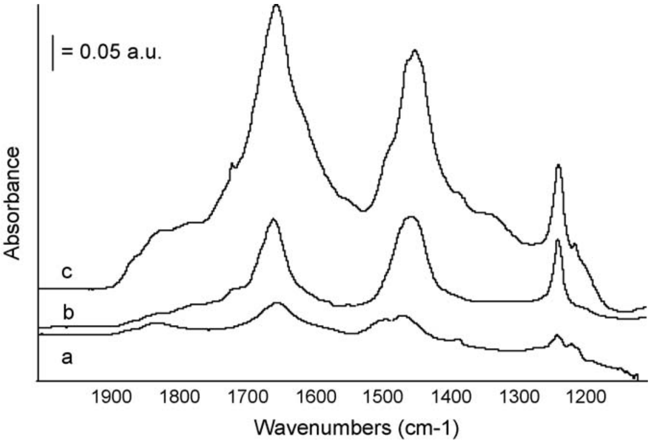

**Fig. 6.** FT-IR spectra of the surface species arising from $CO_2$ adsorption at room temperature over SOX (a), POX (b) and POXL3 (c). Activated surface spectra and gaseous $CO_2$ spectrum have been subtracted.

at 2300 $cm^{-1}$, a sharp band readily disappearing following outgassing at room temperature (not reported here).

Also in spectrum in Fig. 6b ($CO_2$ over POX sample) the detection of three bands at 1650, 1446 and 1231 $cm^{-1}$, strong and quite broad, points out the formation of hydrogen carbonate species. Bands at higher frequencies (1700–1800 $cm^{-1}$) have been reported also by Vimont et al. [17] due to either organic-like carbonate species or bent $CO_2$ and are strongly reduced following outgassing at room temperature.

The same bands can be detected, by far stronger, in the POXL3 spectrum (Fig. 6c), which is more complex and shows several components likely due to a mixture of carbonate (under the form of bidentate and bridging species) and hydrogen carbonate species. Correspondingly, in the high frequency region, a sharp band appears at 3615 $cm^{-1}$, assigned to OH stretching mode of adsorbed hydrogen carbonate species. A shoulder around 1490 $cm^{-1}$ and a weak component around 1400 $cm^{-1}$ have been assigned to the formation of polydentate carbonates, arising from some limited $CO_2$ reaction with the bulk [18].

Although spectra obtained by $CO_2$ adsorption on basic surfaces are quite complex, the band at 1230 $cm^{-1}$ ($\delta$OH of $HCO_3{}^-$ species) has been related to the surface basicity for alumina-based materials [18] and can be taken for the determination of relative basicity of our different metal oxides. Its intensity grows in the order SOX << POX < POXL3 and is the highest in the POXL3 sample, pointing out an increased number of basic sites arising from La-doping of alumina. The integrate intensity of the carbonate complex bands follows the same trend. The reported relative basicity trend, which allows a discrimination among the samples, has to be related with the presence of basic sites strong enough for interacting with $CO_2$ at room temperature (i.e. surface hydroxyls, mainly coordinated to only one cation, and stronger $O^{2-}$ basic sites, where different kind of carbonate species are formed [18,19]).

Surface acidity of the same samples has been studied by PN adsorption. The resulting spectra are reported in Fig. 7, focusing on the CN stretching region. In all the sample spectra two main bands are detected around 2300 and 2237 $cm^{-1}$, the former assigned to PN interaction with Lewis sites, typically $Al^{3+}$ ions characterizing transition alumina [20], the latter due to PN interaction with OH surface groups (H-bonded PN). Following outgassing, the band at 2237 $cm^{-1}$ almost disappears, in agreement with the assignation to a weakly banded species, while the band at 2300 $cm^{-1}$ is still evident. Moreover, the spectrum of PN on POXL3 allows the detection of the two components around 2300 $cm^{-1}$ (PN on Lewis sites) and 2236 $cm^{-1}$ (H-bonded PN) together with a shoulder at 2250 $cm^{-1}$ which is stable to outgassing (Fig. 7c, broken line). This new component can be clearly evidenced in the subtraction result [spectrum c − spectrum b] (Fig. 7, inset) and can be related to CN stretching mode of nitrile adsorbed over metal cations, as reported by Kozyra et al. for nitriles adsorption over Na-zeolites [21]. Thus new Lewis acidic centres are formed at the surface, other than Al. This effect seems to suggest that upon $La_2O_3$ modification, Lewis acidity is increased preferentially, likely related to exposed La coordinatively unsaturated ions which can be detected over a well dispersed lanthanum modified alumina [22–24].

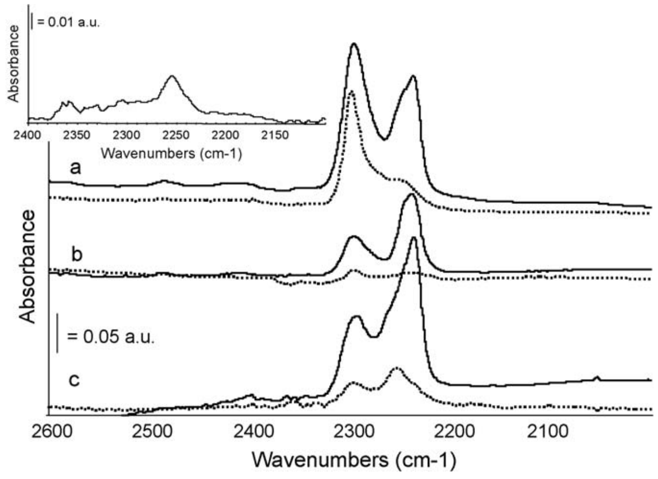

**Fig. 7.** FT-IR spectra of the surface species arising from 1 torr PN adsorption over SOX (a), POX (b) and POXL3 (c). Full line: Spectra recorded at room temperature in the presence of PN; broken line: spectra recorded following desorption at room temperature for 30 s. *Inset*: [spectrum c − spectrum b].

In conclusion, FT-IR characterization of the SOX, POX and POXL3 samples points out a more complex surface situation than that determined by acid titration.

Different surface charging can be related to the different amount of surface basic sites, as revealed by $CO_2$ adsorption over basic surface hydroxyl, leading to hydrogen carbonate species formation, and over basic oxygen ions, leading to carbonate species formation. All these sites can be titrated by $HNO_3$ aqueous solution. In particular, a clear difference can be evidenced, following $CO_2$ adsorption, between SOX and POX/POXL3 samples, in agreement with results from titration with $HNO_3$.

POX and POXL3 samples, which show almost identical behaviours with respect to titration with a strong acid such as $HNO_3$, can be easily discriminated by infrared analysis of adsorbed species. Clearly, modification of the POXL3 surface with La ions results in an increase of the strongest basic sites able to interact with $CO_2$ at room temperature (i.e. oxygen ions and oxygen ions in a lower coordination state). On the other side, $HNO_3$ aqueous solution can buffer the strongest basic sites on POXL3 sample and both these effects should explain the similar surface charging values reported for POX and POXL3 materials in Table 3.

The effect of La doping of alumina also results in the formation of new surface Lewis sites detected by PN adsorption, which could also play a role in modulating the total surface acidity. Thus, for a complete description of the surface both techniques have to be considered and this will become fundamental in the presence of a catalytically active phase, typically a metal or a metal oxide.

## 4. Conclusions

With the purpose of rationalizing the process conditions to be used in the washcoating of structured supports, correlations have been searched between easily measurable physico-chemical properties of the dispersed powders and the final rheology of the adopted slurries.

Simple materials, widely adopted as catalyst carriers, have been employed in this study. It has been found that the rheological properties of the typical suspensions used for the washcoating process can be predicted and controlled *a priori* by knowing the pore volume and the nature of the surface of the dispersed powders. In particular, the maximum surface charging, determined according to surface titration with a strong acid such as $HNO_3$, has been found to be a good parameter to be used for the definition of the amount of dispersant to be added in the slurry.

In order to prepare suspensions with the same rheology but containing powders of different composition, water has to be modulated considering the pore volume, while the acid has to be added on the basis of the maximum surface charging. This is because the relevant parameters controlling the viscosity of the suspensions are the amount of free water and the charge of each suspended particle.

FT-IR analysis of adsorbed $CO_2$ and PN have allowed a more sensitive characterization of surface sites, evidencing that the nature of the surface of the adopted materials is complex, and visibly affected by the presence of a doping agent.

## References

[1] P. Avila, M. Montes, E.E. Mirò, Chem. Eng. J. 109 (2005) 11–36.
[2] A.G. Ersson, S.G. Jaras, Structured Catalysts and Reactors, second ed., Taylor & Francis, Boca Raton (USA), 2006, pp. 215–241, Chapter 7.
[3] I. Nova, A. Beretta, G. Groppi, L. Lietti, E. Tronconi, P. Forzatti, Structured Catalysts and Reactors, second ed., Taylor & Francis, Boca Raton (USA), 2006, pp. 171–214, Chapter 6.
[4] G. Groppi, E. Tronconi, Catal. Today 105 (2005) 297–304.
[5] G. Groppi, C. Cristiani, A. Beretta, P. Forzatti, in: P. Barbaro, C. Bianchini (Eds.), Catalysis for Sustainable Energy Production, Wiley-VCH, Weinheim, 2009, , pp. 363–392, Chapter 12.
[6] R. Guettel, U. Kunz, T. Turek, Chem. Eng. Technol. 5 (2008) 746–754.
[7] M. Valentini, G. Groppi, C. Cristiani, M. Levi, E. Tronconi, P. Forzatti, Catal. Today 69 (2001) 307–314.
[8] T.A. Nijhuis, A.E.W. Beers, T. Vergunst, I. Hoek, F. Kapteijn, J.A. Moulijn, Catal. Rev. Sci. Eng. 43 (4) (2001) 345–380.
[9] C. Cristiani, M. Valentini, M. Merazzi, S. Neglia, P. Forzatti, Catal. Today 105 (2005) 492–498.
[10] C. Brinker, G.W. Scherrer, Sol–Gel Science, Academic Press, NY, 1990.
[11] W.T. de Janusz, Encyclopaedia of Surface and Colloid Science, Marcel Dekker, New York, 2002, pp. 1687–1703.
[12] C. Cristiani, A. Grossale, P. Forzatti, Top. Catal. 42–43 (2007) 455–459.
[13] G. Busca, V. Lorenzelli, G. Ramis, R.J. Willey, Langmuir 9 (1993) 1492–1499.
[14] J.W. Cui, F.E. Massoth, N.-Y. Topsoe, J. Catal. 136 (1992) 361–377.
[15] A.A. Tsyganenko, J. Lamotte, J.P. Gallas, J.C. Lavalley, J. Phys. Chem. 93 (1989) 4179–4183.
[16] T. Yang, L. Feng, S. Shen, J. Catal. 145 (1994) 384–389.
[17] A. Vimont, J.C. Lavalley, A. Sahibed-Dine, C. Otero Arean, M. Rodriguez Delgado, M. Daturi, J. Phys. Chem. B 109 (2005) 9656–9664.
[18] J.C. Lavalley, Catal. Today 27 (1996) 377–401.
[19] A.S. Ivanova, B.L. Moroz, E.M. Moroz, Yu.V. Larichev, E.A. Paukshtis, V.I. Bukhtiyarov, J. Solid State Chem. 178 (2005) 3265–3274.
[20] G. Busca, Phys. Chem. Chem. Phys. 1 (1999) 723–736.
[21] P. Kozyra, I. Salla, T. Montanari, J. Datka, P. Salagre, G. Busca, Catal. Today 114 (2006) 188–196.
[22] L. Sun, X. Guo, M. Liu, X. Wang, Appl. Catal. A: Gen. 355 (2009) 184–191.
[23] H. Vidal, S. Bernal, R.T. Baker, D. Finol, J.A. Perez Omil, J.M. Pintado, J.M. Rodriguez-Izquierdo, J. Catal. 183 (1999) 53–62.
[24] L.P. Haack, J.E. deVries, K. Otto, M.S. Chatta, Appl. Catal. A: Gen. 82 (1992) 199–214.